Study of the Morphology and Kinetics of Novel Ziegler–Natta Catalysts for Propylene Polymerization

Mohammed Abboud,[1] Peter Denifl,[2] Karl-Heinz Reichert[1]

[1]*Institute of Chemistry, Technical University of Berlin, Strasse des 17. Juni 124, D-10623 Berlin, Germany*
[2]*Borealis Polymers Oy, P.O. Box 330, FIN-06101 Porvoo, Finland*

Received 30 December 2004; accepted 1 March 2005
DOI 10.1002/app.22412
Published online in Wiley InterScience (www.interscience.wiley.com).

ABSTRACT: The morphological and kinetic characteristics of novel Ziegler–Natta catalysts were studied. Catalysts were prepared by Borealis Polymers Oy using a new synthesis technique (emulsion technology). Video microscopy was used to study the growth of single catalyst particles during polymerization in the gas and liquid phases. The distribution of single particle activity was very narrow in the catalyst without external support and was rather broad in the the silica-supported catalyst. Video microscopy of molten polymer particles allowed observation of the process and degree of fragmentation of the catalyst particles. A correlation between the activation period during the initial stage of polymerization and catalyst fragmentation was found. Fragmentation was faster and more uniform with the catalyst without external support than with the silica-supported catalyst. Scanning electron microscopy provided information on morphology evolution and shape replication of the catalyst particles. With the catalyst without external support, good shape replication was observed, and compact and spherical particles were formed. With the silica-supported catalyst, shape replication was poor, and nonspherical porous polymer particle were formed. Modeling of the kinetics of propylene polymerization was done using a simple three-step reaction scheme neglecting mass and heat transport effects. © 2005 Wiley Periodicals, Inc. J Appl Polym Sci 98: 2191–2200, 2005

Key words: Ziegler-Natta polymerization; poly(propylene) (PP); morphology

INTRODUCTION

Results of polymerization studies of α-olefins using supported catalysts on fragmentation of catalyst support, replication of particle morphology, and modeling of particle growth have been reported in several articles, for example, those of Kakugo et al. and Chiovetta. Experimental studies and modeling were based on characterization of the morphology of the catalyst and the polymer particles applying microscopy techniques such as SEM and TEM and X-ray techniques, as well as BET measurement and mercury porosimetry.[1]

The morphology of the supported catalysts used in olefin polymerization has a significant influence on polymerization. McDaniel[2] studied the activity of supported polymerization catalysts as a function of porosity and changes in morphology. He showed that catalysts possessing higher porosity showed higher polymerization activity. This was not observed in the Ziegler–Natta catalysts prepared using an emulsion technology, which showed that high activity could also be achieved without having a high degree of porosity.[3–6]

It has been well documented in the literature that growing polymer particles act as individual microreactors and can have their own mass and heat balances. The morphology of polymer particles was found to be a replicate of the catalyst particle morphology.[7–8] In general, good replication of catalyst particles takes place with a uniform polymerization rate, which is the result of homogeneous distribution of the active complex among the catalyst particles as well as the absence of concentration and temperature gradients within the reacting particles.[9–13] If requirements for shape replication are not fulfilled, growing polymer particles can suffer from morphological deformations and particle rupturing could result, causing a complete loss of the original shape.[14]

In general, catalyst fragmentation depends mainly on two factors: hydraulic pressure generated by the formed polymer inside the catalyst pores and the rigidity of the support material.[15] The support must have a mechanical strength great enough to withstand handling and low enough to break down during polymerization.[16] Several published articles have explained the fragmentation of different catalyst systems. Chiovetta studied the fragmentation of catalysts in detail.[17–19] Ferrero and Chiovetta studied the effects of catalyst morphology and fragmentation on the po-

Correspondence to: Mohammed Abboud (m.abboud@chem.tu-berlin-de).
Contract grant sponsor: Borealis Polymers Oy.

lymerization process.[20,21] In studies that used computer simulation to investigate heterogeneous Ziegler–Natta propylene catalysts, it was found that fragmentation occurred as a sequential formation of concentric onion-skin type layers containing solid fragments surrounded and linked by polymer molecules. According to Chiovetta, the sequential formation of concentric layers takes place if the the pores in the catalyst support are, on average, small in size.[18] The fast reaction rate causes rapid accumulation of polymer in the outermost portions of the macroparticle and continues gradually toward the interior of the pellet. Chiovetta also considered another model for a catalyst support rich in mesopores. In this model, the initial support/catalyst particles break first, according to the distribution of their large pores, into a certain number of fragments, which become smaller until they reach a final catalyst fragment size (FCF).

For industrial gas-phase, slurry, or bulk polymerization, it is very essential to support the active catalytic components on a support (drop-in technology) in order to achieve a product with a defined morphology.[22] The type of catalyst support affects the overall activity and activity profile of heterogeneous catalysts and determines the type of catalyst fragmentation.[23–25] $MgCl_2$, as a support for polymerization catalysts, fragments much more extensively at low polymer yields than does as an SiO_2 support. $MgCl_2$ as a support is believed to consist of agglomerations of small crystalline subparticles that are more loosely aggregated than they would with SiO_2.[16]

The current study found a correlation between catalyst morphology and type of support with reaction kinetics, which is detailed in this article. In addition, the particle growth process for a Ziegler–Natta catalyst without an external support and for a silica-supported Ziegler–Natta catalyst, especially in the initial stages of polymerization, is presented, along with a comparision of the morphology and fragmentation behavior of the original catalyst particles with those of the polymer produced. Also, the distribution of the activity of single catalyst particles in both systems along with the overall catalyst activity profile is shown.

EXPERIMENTAL

Polymerization setup

Propylene polymerization both in the gas phase and in slurry was carried out in a special minireactor (reactor volume 100 mL) constructed by Premex AG, Switzerland. The temperature is controlled with a jacket thermostat and the gas pressure with a gas controller connected to the gas cylinder. The polymerization setup as well as an analysis of the microscopic pictures were reported previously.[23–24]

TABLE I
Specifications of Different Catalysts Used for Propylene Polymerization

Catalyst	Cat E	Cat B
Ti (wt %)	3.0	2.7
Mg (wt %)	10.2	6.0
External support	—	silica
Average particle size	23 μm	57 μm

Catalyst system

The catalysts studied were prepared with a novel catalyst preparation technique developed by Borealis Polymers Oy. The new synthesis route is based on an emulsion system. The first stage consists of *in situ* formation of a liquid/liquid two-phase system in which one phase is a solution of the catalyst components or its precursor ($TiCl_4$, magnesium alkoxide, internal donor) in an inert solvent. The second stage is the emulsification, which is performed using a special kind of surfactant for stabilizing the catalyst droplets. At this stage particle size and the size distribution of the final catalyst already have been determined by the mixing conditions. The final stage of the route is solidification of the catalyst droplets. This is performed simply by changing the reaction conditions of the emulsion system. Subsequently, catalyst particles are isolated and dried. The catalyst particles so obtained are characterized by an extremely small surface area (under the detection limit of BET), particles of perfectly spherical shape, and a narrow distribution of particle size.[3–6] The catalyst produced is referred to in this article as nonsupported catalyst because it did not contain an external support. Also prepared was another catalyst that was supported on silica and was based on the same catalyst chemistry. The silica used for catalyst support came from Grace Davison (55SJ, SYLOPOL). Triethyl aluminum (TEA) was used as the cocatalyst. The internal donor was di-(2-ethyl-hexyl) phthalate, and the external donor was dicyclo pentyl dimethoxy silane (D-donor). In all the polymerization experiments performed, the molar ratios of Al : Ti and Al : Si were kept constant at 250 and 10, respectively. The specifications of the different catalyst systems are shown in Table I.

Materials

All sample preparations for microscopic analysis were conducted in a glove box under an N_2 atmosphere with an O_2/H_2O content of less than 1 ppm. Propylene gas with a purity of 3.5 (>99.95 vol %) with propane as the major impurity was purchased from Messer–Griesheim (Germany) and was used without further purification. Pentane and heptane were purified by drying over sodium and distillated under nitrogen.

TEA of 96% purity was purchased from Merck (Germany).

Catalyst activation and polymerization procedure

Around 5 mg of catalyst was weighed and introduced into a septa bottle containing a solution of TEA/ext. donor/pentane previously complexed for 5 min. The suspension was gently shaken for 4 min, and then solids were allowed to settle out for an additional minute. Then the activation solution was removed, and activated catalyst particles were dried. As a result, a fine, darkly colored powder of the activated catalyst was obtained. Meanwhile, a scavenger solution was prepared consisting of TEA/ext.donor/heptane.

A small amount of the activated catalyst particles (<1 mg) was spread on the table for video microscopic measurements. Some drops of the scavenger solution were introduced above the particles. The rest of the catalyst particles were placed on the bottom of the reactor for overall activity measurements. and the rest of the scavenger solution was added. The reactor was then closed, taken out of the glove box, and connected to the gas line. The time needed for the reactor to reach reaction temperature was around 4 min, during which a prepolymerization step occurred. Experiments were performed at a total propylene pressure of 5 bar and a reaction temperature of 25°C–80°C. No hydrogen or comonomer was used, and the reacting particles were not mixed during the polymerization reaction.

Slurry polymerizations also were performed in the minireactor equipped with a magnetic stirrer. Heptane was used as a solvent, and the polymerization reactions were performed at a propylene pressure of 5 bar and a reaction temperature of 45°C in the absence of hydrogen and comonomer.

Analytical methods

Video microscopy (VM)

During the course of polymerization, pictures of growing catalyst particles were gathered and evaluated using picture analysis software.[23,24] Relative volume growth factors (volumes of the polymer particles divided by the original volumes) of individual catalyst particles were determined in order to study the activity distribution and growth behavior of single catalyst particles. More than 100 particles were analyzed for particle growth measurements,.

Video microscopy of polymer melt was employed to study the fragmentation of the support/catalyst particles. The polypropylene samples were first placed on the microscope stage and fixed in a metal ring. They were then heated to 170°C (above the melting point). The temperature was held constant for some minutes, during which melting and crystallization of polymer was monitored.

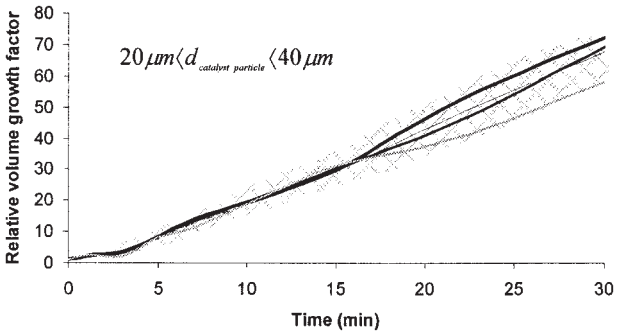

Figure 1 Growth in volume (relative to initial volume) of four randomly selected catalyst particles. The shaded area represents the growth characteristic of 100 particles. Polymerization was performed using the nonsupported Ziegler–Natta catalyst (Cat E) in gas phase at a propylene pressure of 5 bar and a temperature of 45°C.

Scanning electron microscopy (SEM)

Video microscopy in connection with scanning electron microscopy (SEM) allowed deeper insight into the detailed microstructure of the polymer particles, where important structural and morphological information could be gained. Catalyst particles as well as polymer particles produced at different polymerization times were studied. Samples were mounted on aluminum stubs via double-sided conductive carbon tape and sputter-coated with gold to make them conductive. Special care was taken during the sample preparation to study catalyst particles because of reactions of the catalyst with air, causing shape deformation and production of cracked particles covered with a layer of foam. Pictures were taken with a Hitachi S-2700 at various magnification levels.

Microanalysis (EDX)

EDX microanalysis was performed at different points on catalyst particles as well as on low-yield polymer particles. The abundance of titanium was investigated in order to check the distribution of titanium.

RESULTS AND DISCUSSION

Activity of single catalyst particles

An important advantage of video microscopy is its ability to quantitatively measure particle growth. It can describe the growth and startup behavior of individual catalyst particles. Figure 1 shows an example of the relative volume growth of a few randomly selected catalyst particles of different initial sizes produced during the gas-phase propylene polymerization with

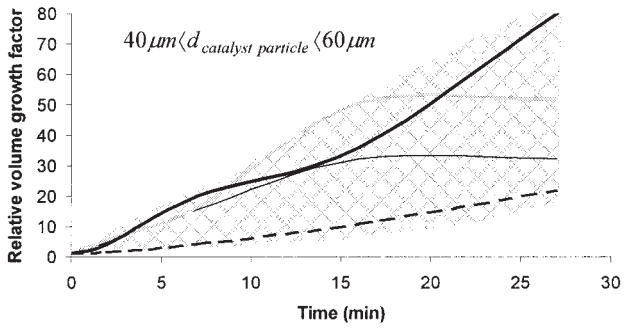

Figure 2 Relative volume growth (relative to initial volume) of four catalyst particles. The shaded area represents the growth characteristic of 100 particles studied. Polymerization was performed using the silica-supported Ziegler–Natta catalyst (Cat B) in the gas phase at a propylene pressure of 5 bar and a temperature of 45°C.

the nonsupported Ziegler–Natta catalyst (Cat E). The shaded area represents the growth characteristics of 100 catalyst particles and shows a similar and steady growth of the particles starting from time zero and continuing through the entire reaction period (30 min).

In contrast, catalyst particles of silica-supported Ziegler–Natta catalyst (Cat B) exhibited a very different growth behavior. Most catalyst particles started to grow immediately after monomer exposure, some particles started growing after a certain period of inhibition, and a very small fraction of catalyst particles did not show growth at all. It is important to mention that the observed induction period for some catalyst particles lasted a few minutes but not longer, as has been observed for some polymerization catalysts supported on silica.[25–26] Figure 2 shows an example of the growth of a few catalyst particles that were selected to show the broad distribution of activities of single catalyst particles. The shaded area represents the growth characteristics of 100 catalyst particles. Possible reasons for the differences in growth behavior include the heterogeneity of the porosity or rigidity of the support concerning or heterogeneous distribution of the active complex among different catalyst particles. Some catalyst systems reported in the literature had single particle activity that was found to depend on particle size (larger particles were shown to be more active).[26] This was not found for the catalyst system used in the present study, which showed no trend in particle activity and particle size. The difference in findings could possibly be explained by differences in the chemistry of the catalyst, in the support properties (porosity, rigidity, etc.), in the catalyst supporting method, and in the reaction conditions.

A small degree of scattering in growth of single catalyst particles was observed, mainly because of error in picture evaluation, which was magnified upon conversion of the apparent area to volume and was therefore not a real effect.

Distribution of catalyst elements

Homogeneous distribution of the active complex in the catalyst particles is a condition for good shape replication. Titanium, the element involved in active site formation, was investigated using EDX microanalysis (point analysis). Analysis was executed on different spots of the same catalyst particle and among different catalyst particles for both the nonsupported and silica-supported catalysts. The results showed similar concentrations of titanium, indicating a rather homogeneous distribution of the active complex. The observed broad distribution of activity of single catalyst particles in the silica-supported Ziegler–Natta is more likely to be a result of the different properties of the support than to problems of active complex distribution among the different catalyst particles.

Because of microscopic limitations, determining titanium concentrations in the polymer particles that had a high polymer/catalyst ratio was not feasible.

Overall activity and activity profile

Simple averaging of the activity of single catalyst particles can be used to study the activity and activity profile of a catalyst system. The mass of polymer particles was calculated on the basis of normalized volumes of polymer particles at different polymerization times and then converted to single particle activities. The density of polypropylene particles produced with the nonsupported Ziegler–Natta catalyst was considered the density of polypropylene because of the compactness of the polymer particles and was assumed to be constant during polymerization. In contrast, the porosity of the polymer particles produced with the silica-supported Ziegler–Natta catalyst was considered in the determination of the density of the polymer particles and also was assumed to be constant during polymerization.

Activities of single particles were averaged and plotted versus time. With the nonsupported Ziegler–Natta catalyst, a fast initial increase in activity (5 min until maximum activity) followed by decay was observed [Fig. 3(a)]. A reason for the fast initial increase could be the rapid catalyst fragmentation. In contrast, the slower fragmentation of the silica-supported Ziegler–Natta catalyst could explain the longer activation period (10 min until maximum activity). Notice that both catalyst systems (Cat E and Cat B) had comparable overall activity. It is worth mentioning that with the nonsupported Ziegler–Natta catalyst, averaging the activities of a small number of catalyst particles was sufficient to study average particle activity. This was because of the narrow activity distribution of single catalyst particles. With the silica-supported Ziegler–Natta catalyst, it was necessary to average the activities of a large number of particles for a

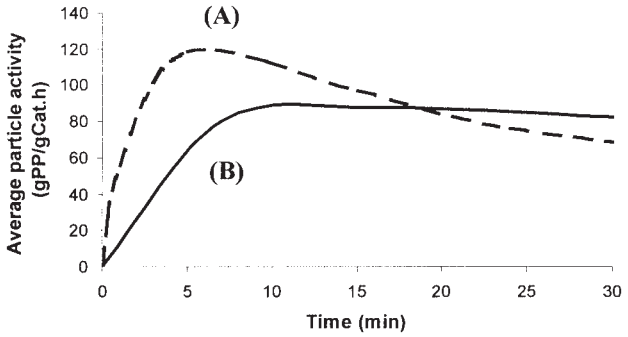

Figure 3 Activity profile determined by video microscopy of (a) nonsupported Ziegler–Natta catalyst (Cat E) and (b) silica-supported Ziegler–Natta catalyst (Cat B). Polymerization was performed in the gas phase at a propylene pressure of 5 bar and a temperature of 45°C.

good determination of catalyst activity because of the broad activity distribution of single particles of this catalyst.

The average particle activity profile determined using video microscopy for the nonsupported Ziegler–Natta catalyst was similar to the overall activity profile measured using a flow meter, excluding the initial stage (Fig. 4). An additional advantage of video microscopy is the ability to study the startup of polymerization (the very first minutes), which is usually not accurately measured using a flow meter.

Catalyst particle morphology

The nonsupported Ziegler–Natta catalyst (Cat E) consisted of spherical particles with smooth surfaces. In contrast, the particles of the silica-supported Ziegler–Natta catalyst (Cat B) were nonspherical and had rough and cracked surfaces (Fig. 5).

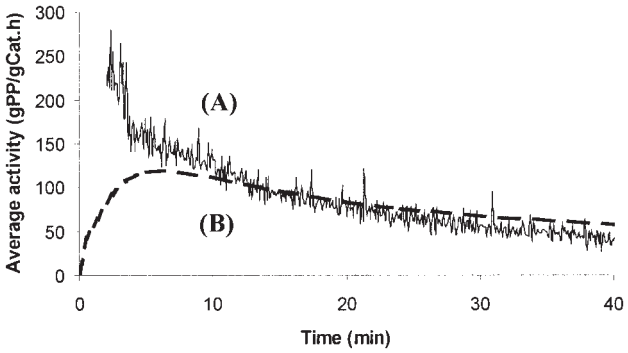

Figure 4 Activity profile measured by (a) flow meter and (b) video microscopy for the gas-phase propylene polymerization with the nonsupported Ziegler–Natta catalyst (Cat E). Polymerization was performed under similar reaction conditions.

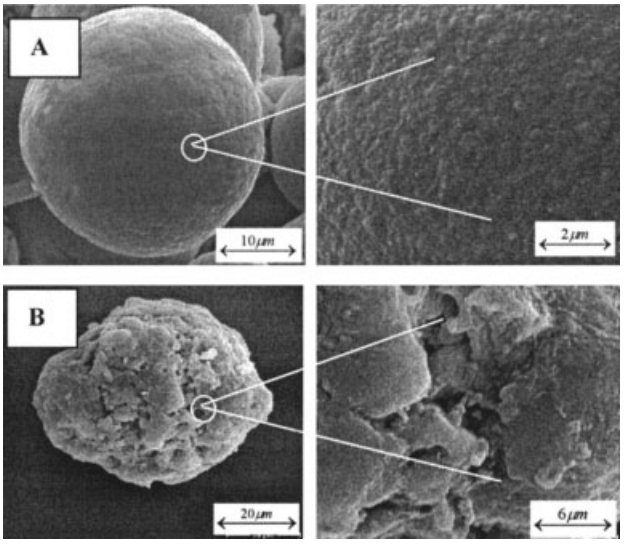

Figure 5 SEM images of catalyst particles of the (a) nonsupported (Cat E) and (b) silica-supported (Cat B) Ziegler–Natta catalysts (not activated).

Particle morphology evolution

SEM pictures taken of polymer particles at different polymerization times (0, 0.5, 10, and 60 min) offered information on the evolution of the morphology of the polymer particles. Most informative were pictures taken of polymer particles polymerized for a short time because initial morphological changes have a major effect on the morphology and microstructure of a mature polymer particle.

In the initial stage of polymerization using the nonsupported Ziegler–Natta catalyst, catalyst particles showed a clear change in morphology. Polymer globules started to form on the catalyst surface (Fig. 6). In the initial stage and under severe reaction conditions (high temperature and/or pressure, slurry or gas phase), the catalyst particle already showed an open structure at the beginning of polymerization (Fig. 7).

During the initial stage of polymerization with the silica-supported Ziegler–Natta catalyst, undefined cracking took place for all the polymer particles stud-

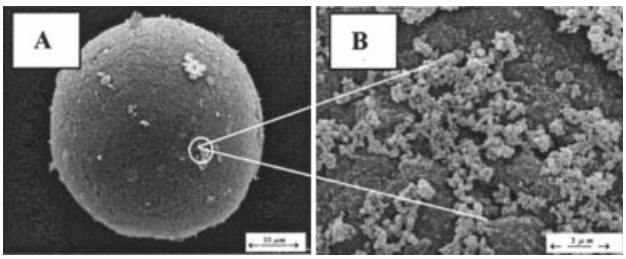

Figure 6 Initial microstructural changes of the nonsupported Ziegler–Natta catalyst (Cat E): (a) catalyst particle after 20 s of polymerization, (b) polymer globules 500 nm–1 μm in size formed at the catalyst surface.

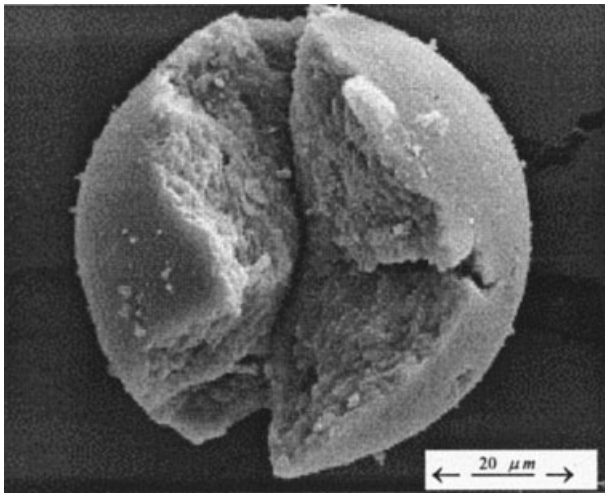

Figure 7 A catalyst particle shortly after polymerization (20 s) showing an open structure [polymerization with the nonsupported Ziegler–Natta catalyst (Cat E) performed at a propylene pressure of 5 bar and a temperature of 80°C].

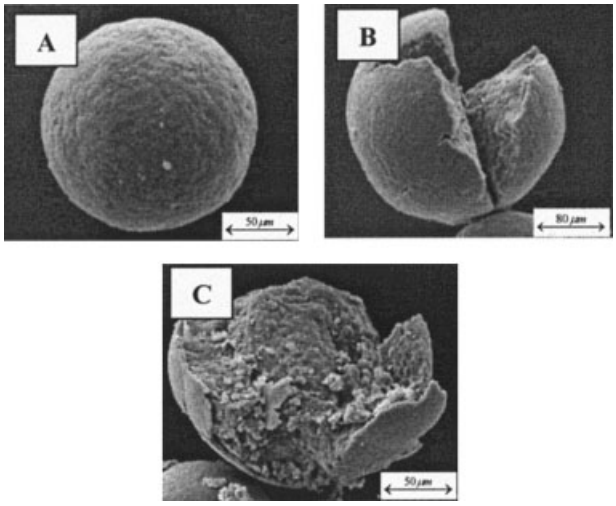

Figure 8 SEM images of polypropylene particles produced by the nonsupported Ziegler–Natta catalyst (Cat E).

ied. First, monomer reached the most accessible active sites, and polymer started to form at the pore throats. This led to hydraulic tension on the pore walls, causing the fracturing of the original support particle. The first formed fractures propagated inside the whole support matrix. Because of heterogeneity of the rigidity or porosity of a particle, fragmentation might occur with different intensities in different parts of the particle, leading to the production of catalyst fragments of very different sizes. SEM images of polypropylene particles produced with SiO_2 supported catalysts in the literature were similar to those produced with the studied silica-supported Ziegler–Natta catalyst.[25]

Polymer particle morphology

Nonsupported ziegler–natta catalyst

Studies performed on polypropylene particles produced with the nonsupported Ziegler–Natta catalyst exhibited either a spherical or a broken spherical structure (Fig. 8).

The different morphologies could be found with varying frequencies based on the reaction conditions and polymerization technique. Under mild reaction conditions (low temperature and pressure), the nonsupported Ziegler–Natta catalyst (Cat E) produced a perfect replication of the shape of the spherical catalyst particles [Fig. 8(a)]. Under more severe reaction conditions (high temperature and/or high pressure), no replication of catalyst morphology took place, and only particles of broken structures were produced [Fig. 8(b,c)]. The nonreplicated shapes were already observed at the very beginning of polymerization, possibly a result of the thermal runaway of growing particles during the initial stage of polymerization, when reacting particles were most sensitive to overheating. A prepolymerization step (low temperature and/or pressure in the initial stage) increased the chance of having good shape replication. Prepolymerization can increase the surface area of the reacting particle without the risk of overheating, which allows controlled fragmentation of the catalyst support.[27]

Silica-supported Ziegler–Natta catalyst

Replication of the catalyst morphology was observed for polymer particles produced by the silica-supported Ziegler–Natta catalyst (Cat B). The morphology of the polymer particles was characterized by nonspherical shapes (Fig. 9). The morphology of the polymer particles produced by the silica-supported Ziegler–Natta catalyst (Cat B) was minimally affected by changing reaction conditions. This may be because of the significant porosity of the original catalyst par-

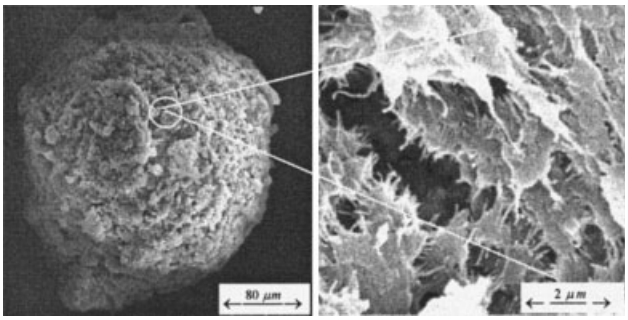

Figure 9 Figure 9 SEM images of polypropylene particles produced by the silica-supported Ziegler–Natta catalyst (Cat B). Polymerization was performed for 1 h in the gas phase at a propylene pressure of 5 bar and a temperature of 45°C.

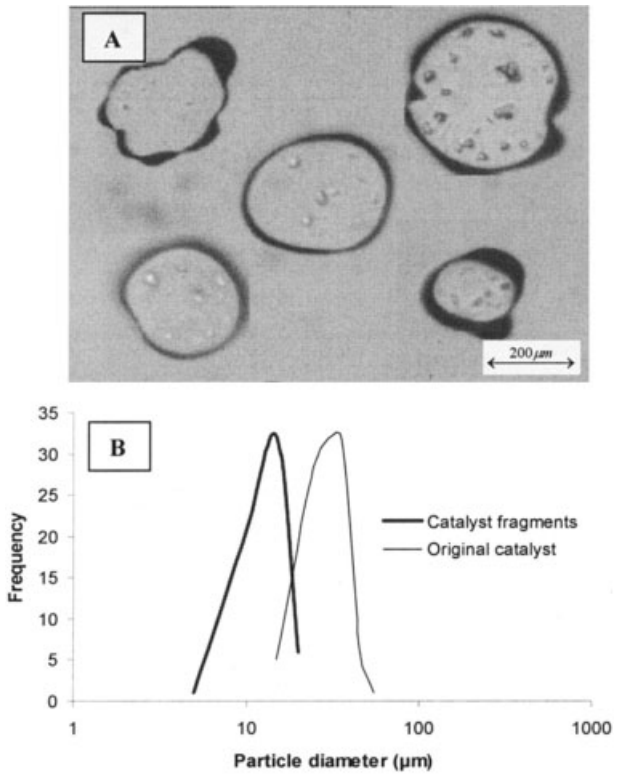

Figure 10 (A) Light microscope image of molten polypropylene particles showing catalyst fragments inside the melt. Polymer particles produced by gas-phase polymerization with the nonsupported Ziegler–Natta catalyst (Cat E) at low-level activity after 10 min of polymerization at a propylene pressure of 5 bar and a temperature of 45°C. (B) Size distribution of the original catalyst particles and catalyst fragments after a 10-min polymerization.

ticles and the slower catalyst fragmentation during polymerization, making the particles more flexible and less likely to rupture.

Catalyst particle fragmentation process

The type of fragmentation that occurred in both catalyst systems (Cat E and Cat B) was investigated. It was noted that analyzing polymer particles produced at different polymerization times could provide information about the support breakup rate and degree of fragmentation during polymerization. Figure 10 shows an example of how catalyst fragments were distributed in molten polypropylene particles produced with the nonsupported Ziegler–Natta catalyst. To best observe fragmentation, this polymerization was performed in the absence of scavenger solution (to keep activity as low as possible). Catalyst fragments of the nonsupported Ziegler–Natta catalyst could no longer be observed at the same magnification with polymer particles polymerized for longer times or at a higher activity level. Analysis showed that fragmentation of the catalyst particles was already fast and uniform from the beginning of polymerization and in the whole catalyst matrix (not only from the outside, as had been assumed for some catalyst systems). Fragmentation continued until the catalyst fragments became smallest in size as subunits or subparticles, which remained dispersed and entrapped in the growing polymer mass and acted as a nucleus for further polymer growth. This kind of substantial fragmentation is well documented in the literature, for example in the studies by Buls et al.[28] and, later, by Ferrero et al.,[29] Niegisch et al.,[30] and Kakugo et al.[31,32]

Another advantage of molten polymer analysis is the ability to study the activity distribution of single catalyst particles. This can be demonstrated simply by comparing the degree of support disintegration in different molten polymer particles. With the nonsupported Ziegler–Natta catalyst [Figure 10(a)], polymer particles are characterized by a similar degree of catalyst disintegration, that is, similar activity independent of their size. Catalyst fragments were uniformly distributed in the polymer phase. A large number of molten polymer particles were analyzed and fragment sizes were compared to the initial catalyst particle size. Particle size distribution of catalyst fragments in a short polymerization time with the nonsupported catalyst showed a narrow distribution of fragment sizes [Fig. 10(b)].

Polypropylene particles produced with the silica-supported Ziegler–Natta catalyst also were analyzed. Polymer particles polymerized at a high level of activity (1 h, 5 bar, and 45°C) and then melted showed a different support disintegration behavior [Fig. 11(a)]. Catalyst fragments of different sizes and shapes were found to be distributed inside the polymer particles. This is another indication of the broad activity distribution of single catalyst particles observed for the silica-supported Ziegler–Natta catalyst. Fragmentation of the catalyst was not completed even at a very high polymer yields. On average, around 20% of each catalyst particle remained unfragmented after 1 h of polymerization under these reaction conditions. Sizes of the catalyst fragments also were analyzed and compared to the initial catalyst particle size. The fragment size distribution was found to be rather broad [Fig. 11(b)].

Because of the better detectable fragmentation of the silica-supported catalyst, an intensive study using this catalyst was performed in order to investigate a correlation between catalyst fragmentation and activation period. Surface area, number, and perimeter of the original catalyst particles and fragments (resulting from the same number of catalyst particles) at different polymerization times were investigated. After a short polymerization time, fragmentation started in the whole catalyst matrix [Fig. 12(a)]. Over the course of polymerization the fragments increased in number and their particle size distribution became broader

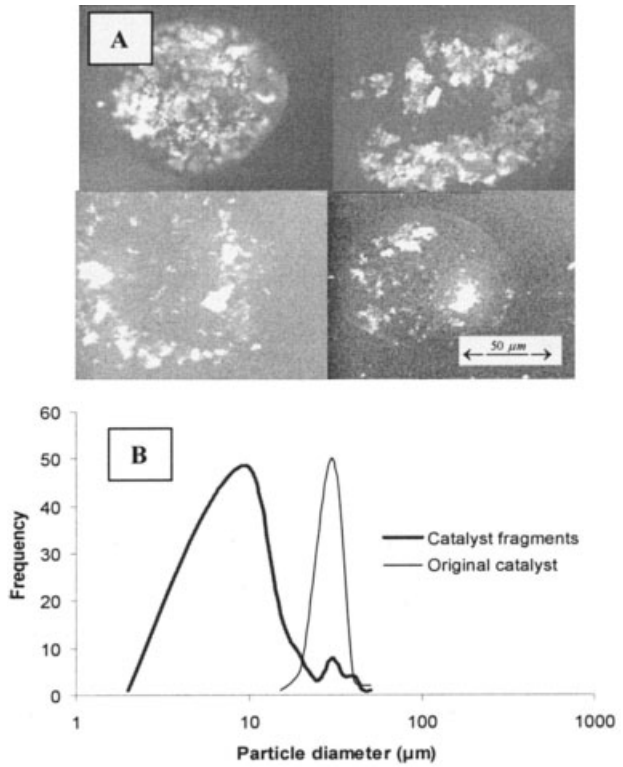

Figure 11 (a) Light microscope image of molten polypropylene particles showing catalyst fragments inside the melt. Polymer particles were produced by gas phase polymerization with the silica-supported Ziegler–Natta catalyst (Cat B) after 1 h at a propylene pressure of 5 bar and a temperature of 45°C. (B) Size distribution of the original catalyst particles and catalyst fragments.

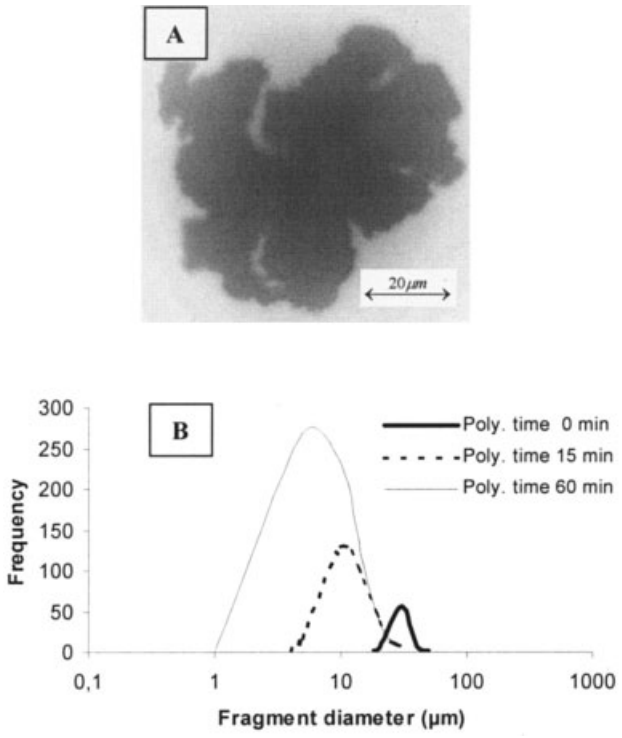

Figure 12 (a) Light microscope image of a polymer particle polymerized for a short time (30 s) and then melted. (B) Frequency of support fragments determined starting from the same number of catalyst particles at three polymerization times (0, 15, and 60 min). Polymerization was performed with the silica-supported Ziegler–Natta (Cat B) at a propylene pressure of 5 bar and a temperature of 45°C.

[Fig. 12(b)]. The original catalyst particles were considered one-fragment particles at time zero, and afterward a continuous increase in fragment number and fragment surface area over the polymerization period studied was observed. The rate of increase of the surface area was found to correspond to the rate of polymerization (Fig. 13). Both showed similar profiles: an initial increase reaching a maximum and then falling during the time studied. The activation period therefore seemed to a great extent to be a physical process.

Modeling of average particle activity of polymerization

The kinetics of catalyst particle activity resulting from video microscopic studies can be modeled by using a simple reaction scheme and neglecting mass and heat transport effects. A simple chemical model was applied without considering physical processes, even though it was shown that catalyst activation was mainly a result of support fragmentation. The model presented is based on that of Bartke[33] and is valid for gas-phase polymerization of propylene with the nonsupported and silica-supported Ziegler–Natta catalysts (Cat E and Cat B). Average particle activity determined using video microscopy at 45°C and 5 bar in the absence of hydrogen or comonomer was simu-

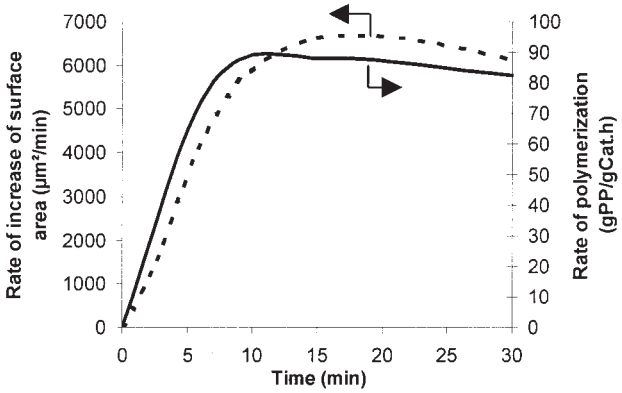

Figure 13 Activity profile of the silica-supported Ziegler–Natta catalyst (Cat B) along with the rate of increase of the surface area of the catalyst fragments. Polymerization was performed at a propylene pressure of 5 bar and a temperature of 45°C.

lated. The model considered one type of active site, monomer participation in active site formation, and a first-order deactivation reaction:

1. Formation of active sites: $Ti + M \xrightarrow{k_i} P_1^*$
2. Chain propagation: $P_n^* + M \xrightarrow{k_p} P_{n+1}^*$
3. Deactivation of active sites: $P_n^* \xrightarrow{k_d} D_n + Ti_{\text{inactive}}$

The analytical solution of the mass balances was:

$$A(t) = 36\frac{M_M k_i k_p C_M^2 X_{Ti}}{(k_d - k_i c_M)M_{Ti}}[\exp(-k_i c_M t) - \exp(-k_d t)]\left[\frac{g_{pp}}{g_{cat}\cdot h}\right]$$

Figure 14 shows the activity, measured by video microscopy, along with the simulated activities of Cat E and Cat B versus reaction time. Fitting was performed by keeping k_p constant and only varying k_i and k_d. The determined rate constants are shown in (Table II).

CONCLUSIONS

This study has shown that a nonporous catalyst may have a high level of activity. Until now, it was believed that a highly porous catalyst was needed in order to achieve high activity.

The synthesis of a catalyst system with a narrow activity distribution of catalyst particles requires a support with the characteristics of homogeneous fragmentation and uniform distribution of the active catalyst complex.

Mass transport effects seemed to play a minor role during polymerization with the novel catalyst system because the activity of catalyst particles was observed to be independent of their size under the reaction conditions studied.

TABLE II
Fitted Kinetic Parameters at 5 bar and 45°C for Both Catalyst Systems

	Rate constants		
Catalyst	k_i (l/mol s)	k_p (l/mol s)	k_d (l/s)
Cat E	3.5×10^{-2}	550	4.0×10^{-4}
Cat B	2.0×10^{-2}	550	1.4×10^{-4}

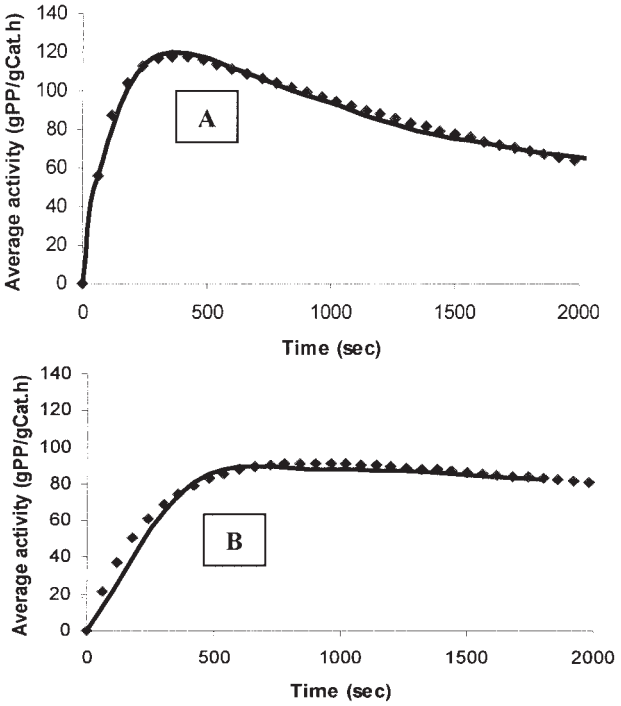

Figure 14 Average particle activity of (a) nonsupported (Cat E) and (b) silica-supported (Cat B) Ziegler–Natta catalysts versus time. Polymerization was performed for 1 h in the gas phase at a propylene pressure of 5 bar and a temperature of 45°C (dots : experiment; line : model).

We thank Dr. Peter Denifl of Borealis Polymers Oy for supplying the catalysts.

References

1. Grof, Z.; Kosek, J.; Marek, M. European Conference on the Reaction Engineering of Polyolefins; Lyon, France, July 2004.
2. McDaniel, M. P. J Polym Sci, Polym Chem Ed 1981, 19, 1967.
3. Denifl, P.; Leinonen, T. EP1273595A1.
4. Pöhler, H.; Denifl, P.; Leinonen, T.; Vestberg, T. MetCon 2003.
5. Denifl, P.; Leinonen, T.; EUPOC 2003, Milan, Italy, 2003.
6. Leinonen, T.; Denifl, P.; Vestberg, T. EUPOC 2003, Milan, Italy, 2003.
7. Hock, C. W. J Polym Sci, Polym Chem Ed 1966, 4, 3055.
8. Boor, J. Ziegler–Natta Catalysts and Polymerizations; Academic Press: New York, 1979.
9. Galli, P.; Noristi, L. Soc Chim Ind, Paris, France, 1978.
10. Galli, P.; Barbe, P. C.; Noristi, L. Presented at the 28th IUPAC Macromolecular Symposium, Amherst, MA, July 12–16, 1982.
11. Bohm, L. Chem Ing Tech 1984, 66, 674.
12. Hutchinson, R. A.; Ray, W. H. J Appl Polym Sci 1991, 43, 1271.
13. Hutchinson, R. A.; Chen, C. M.; Ray, W. H. J Appl Polym Sci 1992, 44, 1389.
14. Karol, F. J.; Wagner, B. E.; Levine, I. J.; Goeke, G. L.; Noshay, A.; Seymour, R. B.; Cheng, T. Plenum: New York, 1987.
15. Weickert, G.; Meier, G. B.; Pater, J. T. M.; Westerterp, K. R. Chem Eng Sci 1999, 54, 3291.
16. Pater, J. T. M.; Weickert, G., Swaaij, W. P. M. J Appl Polym Sci 2003, 87, 1421.
17. Chiovetta, M. G., Ph.D. Dissertation, University of Massachusetts at Amherst, 1983.
18. Chiovetta, M. G. European Conference on the Reaction Engineering of Polyolefins; Lyon, France, 2002.
19. Ferrero, M. A.; Koffi, E.; Sommer, R.; Conner, W. C. J Polym Sci, Polym Chem Ed 1992, 30, 2131.
20. Ferrero, M. A.; Chiovetta, M. G. Polym Eng Sci 1987, 27, 1448.
21. Ferrero, M. A.; Chiovetta, M. G. Polym Eng Sci 1991, 31, 886.

22. Soga, K.; Kaminaka, M. Makromol Chem, Rapid Commun 1992, 13, 221.
23. Abboud, M., Kallio; K., Reichert, K.-H. Chem Eng Technol 2004, 27, 694.
24. Abboud, M.; Patzlaff, M.; Reichert, K.-H. 8th International Workshop on Polymer Reaction Engineering; Dechema Monographien 2004, 138, 197.
25. Steinmetz, B.; Tesche, B.; Przybyla, C., Zechlin, J.; Fink, G. Acta Polym 1977, 48, 392.
26. Knoke, S.; Ferrari, D.; Tesche, B.; Fink, G Angew Chem 2003, 115, 5244.
27. Pater, J. T. M.; Weickert, G.; Swaaij, W. P. M. AICHE 2003, 49(1), 180.
28. Buls, V. H.; Higgins, T. L. J Polym Sci 1970, 8, 1025.
29. Ferrero, M. A.; Sommer, R.; Spanne, P.; Jones, K. W.; Conner, W. C. J Polym Sci, Polym Chem Ed 1993, 31, 2507.
30. Niegisch, W. D.; Crisafulli, S. T.; Nagel, T. S.; Wagner, B. E. Macromolecules 1992, 25, 3910.
31. Kakugo, M.; Sadatoshi H.; Sakai, J.; Yokoama, M. Macromolecules 1989, 22, 3172.
32. Kakugo, M.; Sadatoshi, H.; Yokoama, M.; Kojima, K. Macromolecules 1989, 22, 547.
33. Bartke, M.; Wartmann, A.; Reichert, K.-H. J Appl Polym Sci 2003, 87, 270.